REALIZING A HIGH-INTENSITY LOW-EMITTANCE BEAM IN THE J-PARC 3-GeV RCS

H. Hotchi#, H. Harada, S. Kato, K. Okabe, P. K. Saha, Y. Shobuda, F. Tamura,
N. Tani, Y. Watanabe, and M. Yoshimoto
J-PARC Center, Japan Atomic Energy Agency, Tokai, Naka, Ibaraki, 319-1195 Japan

Abstract

The J-PARC 3-GeV rapid cycling synchrotron is now developing beam studies to realize a high-intensity low-emittance beam with less beam halo. This paper presents the recent experimental results while discussing emittance growth and its mitigation mechanisms.

INTRODUCTION

The J-PARC 3-GeV rapid cycling synchrotron (RCS) is the world's highest class of high-power pulsed proton driver aiming for an output beam power of 1 MW [1-3]. A 400-MeV H^- beam from the injector linac is multi-turn charge-exchange injected into RCS through a carbon foil over a period of 0.5 ms. RCS accelerates the injected protons up to 3 GeV with a repetition rate of 25 Hz. Most of the RCS beam pulses are delivered to the materials and life science experimental facility (MLF), while only four pulses every several second are injected to the following main ring synchrotron (MR). The requirements for the beam operations to MLF and MR are different. Thus, different parameter optimizations are required for each.

Machine activations of RCS are mainly determined by the beam operation to MLF. Hence, sufficient beam loss mitigation has to be achieved in this operation mode. In addition, from MLF, a wide-emittance beam with low charge density is required to mitigate a shockwave on their neutron production target, which is essential to ensure a sufficient lifetime of the target. As already reported in IPAC'16 [4], the requirement for the 1-MW beam operation to MLF was accomplished finally by introducing wide-ranging transverse injection painting with a painting emittance of ε_{tp}=200π mm mrad in combination with betatron resonance correction [5, 6].

On the other hand, from MR, a low-emittance beam with less beam halo is required contrary to the MLF case, which is essential to mitigate beam loss in MR. RCS is now intensively developing high-intensity beam tests (~7.0 x 10^{13} protons per pulse, corresponding to ~84% of the full intensity) to realize such a high-intensity low-emittance beam required from MR. This paper presents the recent experimental results while discussing emittance growth and its mitigation mechanisms.

OPTIMIZATION OF TRANSVERSE INJECTION PAINTING

We first conducted the optimization of transverse injection painting [7] to minimize emittance growth during injection.

#hotchi.hideaki@jaea.go.jp

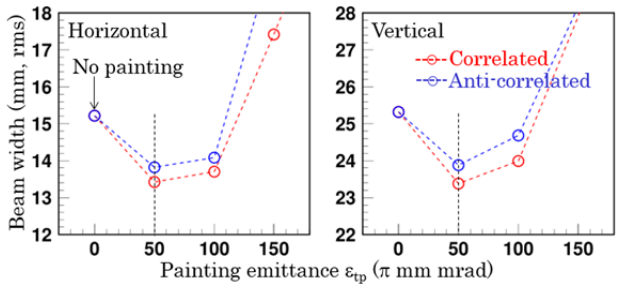

Figure 1: Beam widths at 1 ms right after injection, measured as a function of the painting emittance.

Figure 1 shows the beam widths at 1 ms right after injection, measured as a function of the painting emittance. As shown in the figure, the minimum beam width was achieved for a small painting emittance of ε_{tp}=50π mm mrad. Transverse painting mitigates space-charge induced emittance growth by widely distributing beam particles on the transverse phase space. This painting parameter dependence of beam width is ascribed mainly to the balance of painting emittance and its resultant space charge mitigation. In addition, in the figure, one can find that correlated painting rather than anti-correlated painting provides narrower beam width. This empirical situation can be comprehended by taking into account the effect of the $2\nu_x-2\nu_y=0$ resonance.

The $2\nu_x-2\nu_y=0$ resonance is a 4th order systematic resonance and it is excited mainly by the octupole component in the space-charge field. As is well known, this resonance causes emittance exchange between the horizontal and the vertical planes [8]. This emittance exchange leads to the following two effects, (1) and (2), during the beam painting process.

One (1) is additional emittance growth caused by the direct effect of emittance exchange, which is more enhanced in correlated painting. As shown in the left plot in Fig. 2, in correlated painting, the injection beam is painted along the yellow arrow, namely from the middle to the outside on both the horizontal and the vertical phase spaces. To this direction of beam painting, the emittance exchange occurs in the orthogonal direction, as shown by the red arrow. Therefore, in this case, the emittance exchange is directly connected to emittance growth over the painting area.

Another (2) is additional emittance growth caused by the secondary effect of emittance exchange, namely, by a modulation of the charge density, which is more enhanced in anti-correlated painting. As shown in the right plot in Fig. 2, in anti-correlated painting, the painting process on the vertical plane is reversed; the injection beam is filled

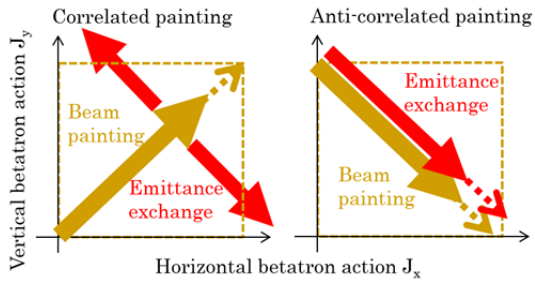

Figure 2: Schematic diagrams of injection painting and emittance exchange.

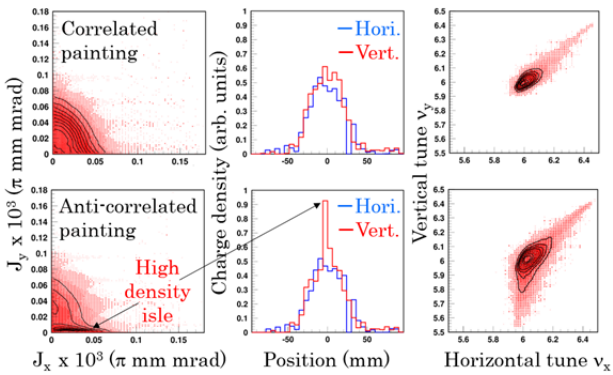

Figure 3: (Left) 2d plots of betatron actions calculated at the end of injection (at 0.5 ms). (Middle) Beam profiles measured at 0.5 ms. (Right) Tune footprints calculated at 0.5 ms.

from the middle to the outside on the horizontal plane, while, from the outside to the middle on the vertical plane. This direction of beam painting is the same as the direction of emittance exchange. Thus, in this case, additional emittance growth caused by the direct effect of emittance exchange is well suppressed. But, this situation causes a significant modulation of the charge density by synchronism between beam painting and emittance exchange, as shown in the lower-left plot in Fig. 3. This characteristic behaviour of charge distribution was confirmed experimentally, as shown in the lower-middle plot in Fig. 3. This high density isle produces large space-charge detuning, as shown in the lower-right plot in Fig. 3, leading to significant emittance growth afterwards.

In the present operational condition, the emittance growth caused by (2) is more critical. Correlated painting avoids the effect. This is the main reason why narrower beam emittance is achieved for correlated painting.

OPTIMIZATION OF TUNE AND CHROMATICITY MANIPULATIONS

Next, we attempted to mitigate additional emittance growth during acceleration after injection.

As is shown later, significant additional emittance growth was observed for the first 6 ms after injection. The numerical simulation conformed the emittance growth is mainly caused by three systematic resonances; $\nu_{x,y}=6$ and $2\nu_x-2\nu_y=0$ (see Fig. 6 shown later). In Fig. 4, one can see

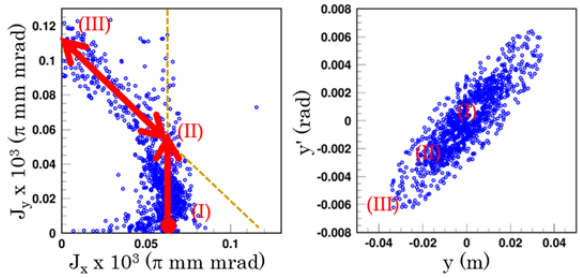

Figure 4: Single-particle behaviour of one macro-particle causing emittance growth. (Left) Turn-by-turn betatron actions. (Right) Transverse phase space coordinates.

	Tune	Chromaticity correction
(A) :	ID 1	Off
(B) :	ID 2	Off
(C) :	ID 2	On (with dc sextupoles)
(D) :	ID 3	On (with dc sextupoles)

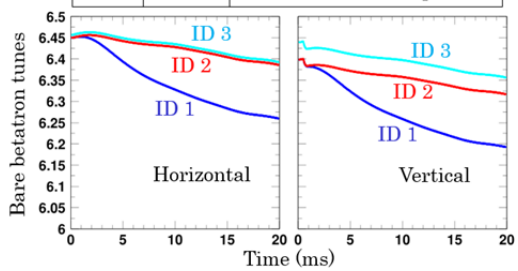

Figure 5: (Upper) Operational parameter settings tested; (A)–(D). (Lower) Tune variations from injection to extraction applied for (A)–(D); ID1–3.

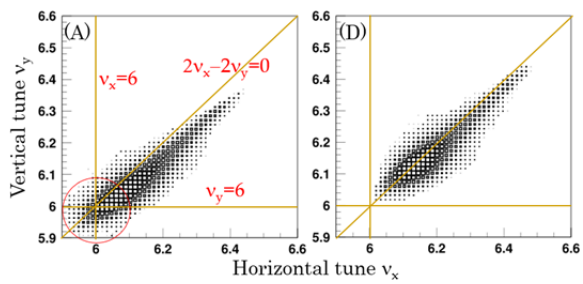

Figure 6: Tune footprints calculated at 4.7 ms.

characteristic emittance growth on the vertical plane caused by the resonances; the emittance growth from (I) to (II) is caused by $\nu_y=6$, and it is further enhanced from (II) to (III) through emittance exchange caused by $2\nu_x-2\nu_y=0$. Similar emittance growth is also generated on the horizontal plane by $\nu_x=6$ and $2\nu_x-2\nu_y=0$.

Based on the above numerical simulation result, we tried to mitigate the emittance growth originating from $\nu_{x,y}=6$. The operational parameter settings tested are listed in Fig. 5. The parameter (A) is the original one, in which the tune is set to ID 1 with no chromaticity correction. In this case, a portion of core particles reaches $\nu_{x,y}=6$ (see left plot in Fig. 6), causing large emittance growth (see blue curves in Fig. 7). To improve this situation, the operational parameter was modified from (A) to (D) step by step. At first, (B) the tune was modified to ID 2, and

ISBN 978-3-95450-182-3

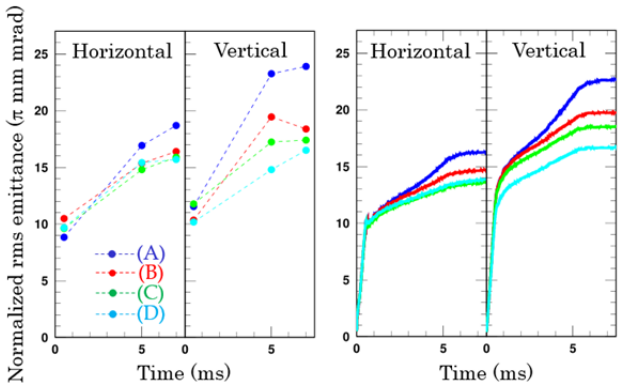

Figure 7: (Left) Normalized rms emittances measured over the first 7 ms. (Right) Corresponding numerical simulation results.

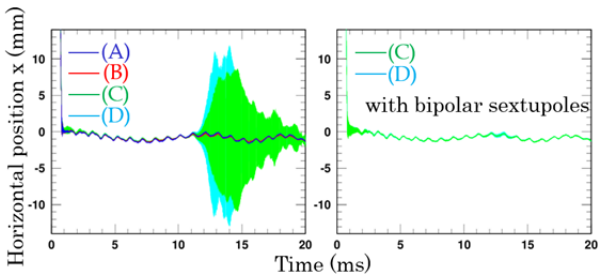

Figure 8: Horizontal beam positions measured over the whole acceleration time of 20 ms.

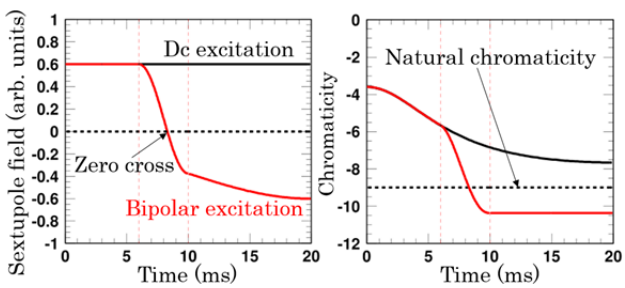

Figure 9: (Left) Sextupole field patterns over the whole acceleration time of 20 ms. (Right) Time dependences of chromaticity.

then, (C) the chromaticity correction was added with dc sextupole fields, and finally, (D) the tune was further modified to ID 3. As shown in Fig. 6, the separation of beam particles from $\nu_{x,y}$=6 is improved in the order from (A) to (D). The experimental results shown on the left side in Fig. 7 confirmed the emittance growth declines in the order from (A) to (D), as predicted by the numerical simulations displayed on the right side in Fig. 7.

But, at this stage, there still remained one issue to be solved for the use of the new parameters (C) and (D). In RCS, the extraction pulse kicker is the most dominant impedance source, causing horizontal beam instability depending on operational parameters [9, 10]. As shown in the left plot in Fig. 8, the parameters (C) and (D) enhance beam instability after 10 ms, whereas they well mitigate emittance growth for the first 6 ms.

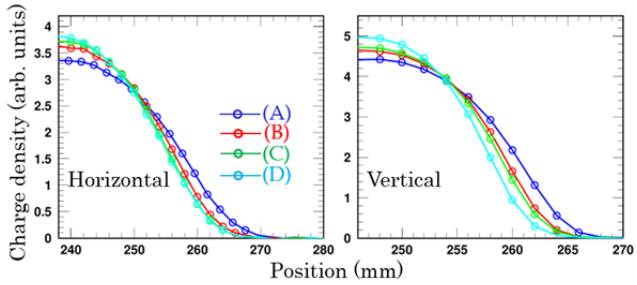

Figure 10: Beam profiles measured at the extraction energy (at 20 ms).

A practical way to solve the beam instability is to dynamically manipulate chromaticity during acceleration, as shown in Fig. 9. In this method, the chromaticity is adjusted to be small for the first 6 ms with dc sextupole fields, which is required for mitigating the emittance growth in this period. Then, after 6 ms, the sextupole fields gradually fall down to zero, and thereafter, they are excited in the opposite polarity to further increase the chromaticity. By this way, the chromaticity after 10 ms is increased by 17% over the natural value. This large negative chromaticity after 10 ms enhances Landau damping through momentum spread, which favours the suppression of beam instability.

In order to realize such a bipolar excitation of sextupole field, we improved the sextupole magnet power supply in the summer maintenance period in 2016. The following beam experiment confirmed that the beam instability is sufficiently damped as expected by this chromaticity manipulation, as shown in the right plot in Fig. 8.

The result of the profile measurements at the extraction energy (at 20 ms) is given in Fig. 10. As clearly shown in the figure, the extraction beam emittance including its tail part was successfully decreased from (A) to (D), where the bipolar sextupole field patterns were applied for (C) and (D). This improvement of the extraction beam quality reflects the emittance growth mitigation achieved for the first 6 ms.

By this success of beam tuning, the beam loss at the beam scraping system located between RCS and MR was drastically reduced to less than half. MR beam tuning with the improved RCS beam is now ongoing.

SUMMARY

For this past year, a large fraction of our effort was focused on realizing a high-intensity low-emittance beam. The extraction beam emittance including its tail part was successfully decreased by optimizing transverse injection painting, and tune and chromaticity manipulations, where bipolar sextupole field patterns were newly introduced to simultaneously achieve emittance growth mitigation at the early stage of acceleration and beam instability suppression after the middle stage of acceleration. In addition, in this work, characteristic behaviours of beam particles during injection painting, appearing coupled with emittance exchange, was revealed.

REFERENCES

[1] High-intensity Proton Accelerator Project Team, JAERI Report *No. JAERI-Tech 2003-044.*
[2] H. Hotchi *et al.*, Phys. Rev. ST Accel. Beams **12**, 040402 (2009).
[3] H. Hotchi *et al.*, Prog. Theor. Exp. Phys. **2012**, 02B003 (2012).
[4] H. Hotchi *et al.*, in *Proc. IPAC'16*, Busan, Korea, 2016, pp. 592−594.
[5] H. Hotchi *et al.*, Nucl. Instrum. Methods Phys. Res., Sect. A **778**, 102 (2015).
[6] H. Hotchi *et al.*, Phys. Rev. Accel. Beams **19**, 010401 (2016).
[7] H. Hotchi *et al.*, Phys. Rev. ST Accel. Beams **15**, 040402 (2012).
[8] B. W. Montague, CERN-Report No. 68−38, 1968.
[9] Y. Shobuda *et al.*, Prog. Theor. Exp. Phys. **2017**, 013G01 (2017).
[10] P. K. Saha *et al.*, in *Proc. IPAC'16*, Busan, Korea, 2016, pp. 589−591.

ISBN 978-3-95450-182-3